

Supporting Information

Orientation-polarization dependence of pressure-induced Raman anomalies in anisotropic 2D ReS₂

Ting Wen¹, Maodi Zhang¹, Jing Li¹, Chenyin Jiao¹, Shenghai Pei¹, Zenghui Wang¹,
Juan Xia¹

¹*Institute of Fundamental and Frontier Sciences, University of Electronic Science and
Technology of China, Chengdu 610054 China.*

Email: zenghui.wang@uestc.edu.cn, juanxia@uestc.edu.cn

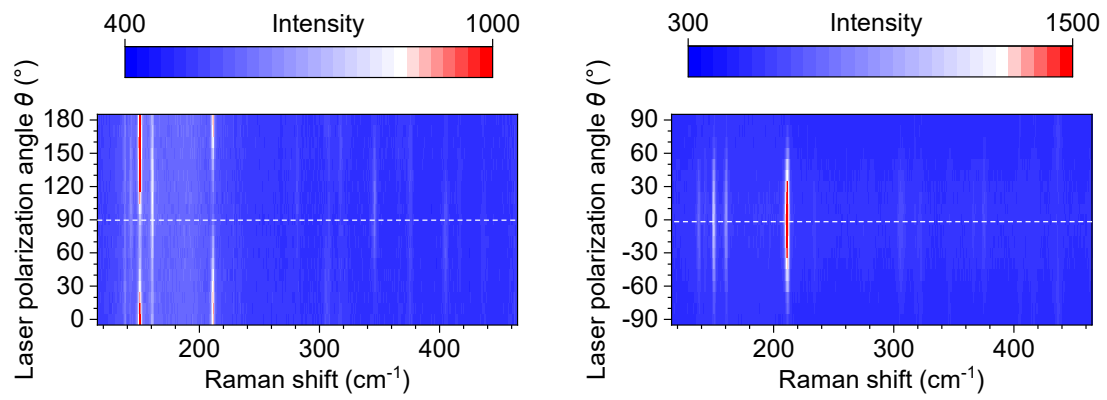


Figure S1. 2D color plots of the angle-resolved Raman spectra of ReS₂ crystals with laser polarization rotated from 0° to 180° under H (a) and V (b) configurations.

Peak	$f(\text{cm}^{-1})$	Mode	Peak	$f(\text{cm}^{-1})$	Mode
1	137	A _g _like	10	305	E _g _like
2	142	E _g _like	11	316	A _g _like
3	150	E _g _like	12	320	A _g _like
4	160	E _g _like	13	344	E _g _like
5	210	A _g _like	14	365	A _g _like
6	232	A _g _like	15	374	E _g _like
7	273	A _g _like	16	403	A _g _like
8	279	E _g _like	17	415	A _g _like
9	303	A _g _like	18	435	A _g

Table S1. Summary and mode assignment of measured Raman intensity of all the 18 Raman active modes in ReS₂ crystal.

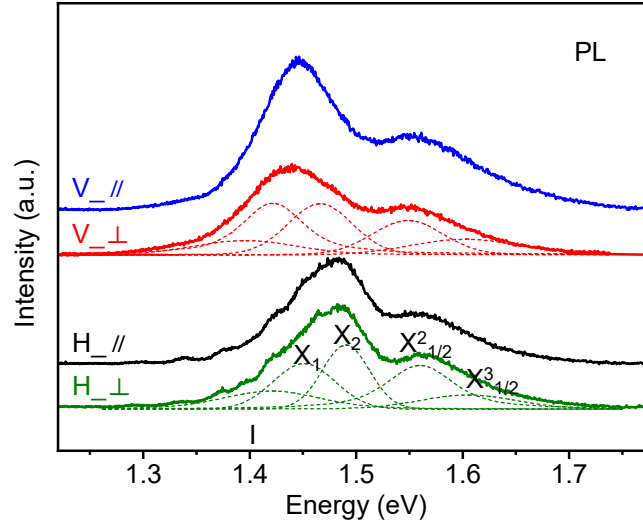


Figure S2 PL spectra of ReS₂ crystal with four representative orientation-polarization configurations at ambient pressure: sample H with laser polarization parallel (H_{//}) and perpendicular (H_⊥) to the ReS₂ crystal *b* axis; and sample V with laser polarization parallel (V_{//}) and perpendicular (V_⊥) to the *b* axis. The dotted curves are fitted by Voigt functions.

the PL peaks are fitted by Voigt functions, consisting of five prominent peaks at 1.42, 1.45, 1.49, 1.56 and 1.60 eV. The peak I corresponds to the lowest-energy indirect transition. The other four peaks are found to originate from two direct excitons (X₁, X₂): peak X₁ and X₂ are the ground state of the two direct excitons corresponding to the recombination emission of excitons along and perpendicular to the Re-Re chain in ReS₂ crystal; peak X²_{1/2} and peak X³_{1/2} are attributed to a nonthermalized hot PL process from direct hydrogenic Rydberg exciton series. The slight difference in PL spectra under H and V configurations could be attributed to the thickness difference in samples and absorption difference among different configurations.

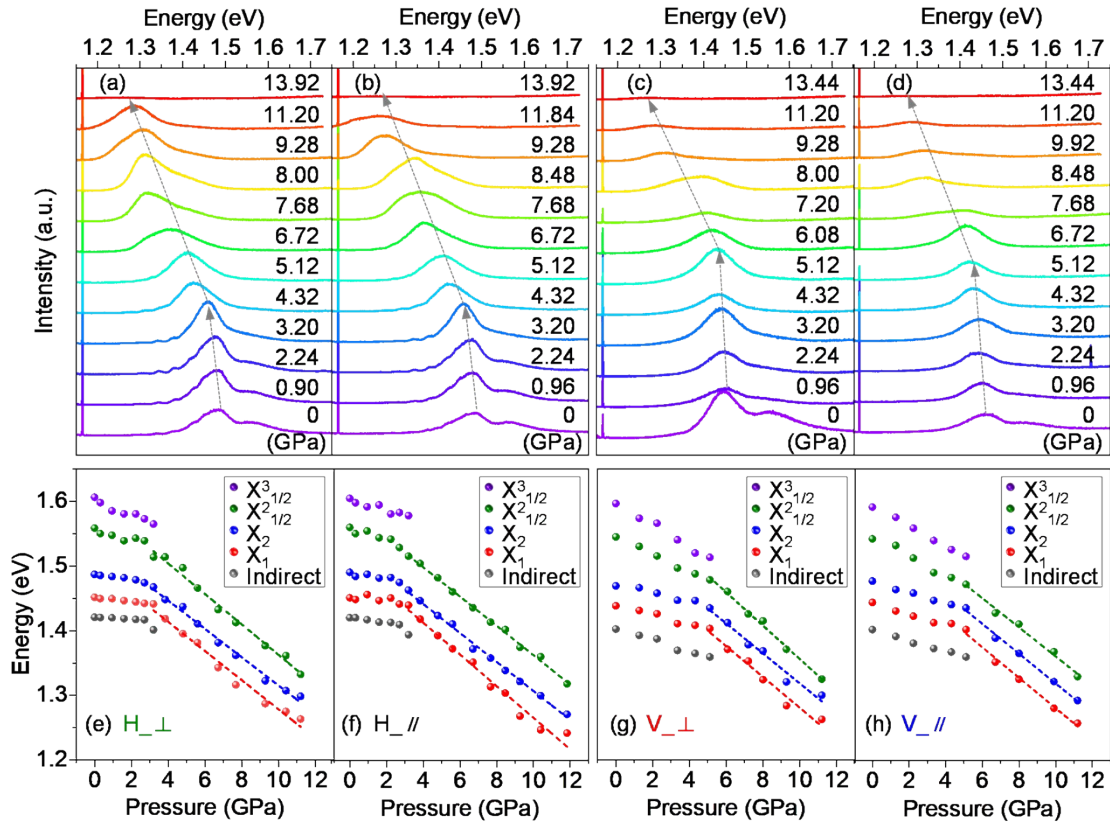


Figure S3 (a)-(d) The evolution of PL spectrum of ReS₂ crystal with pressures (0-14 GPa), for H_{//}, H_⊥, V_{//} and V_⊥ configurations. (e)-(h) The exciton energy of the five PL peaks (see fittings in Figure S2) from data in (a)-(d) as a function of pressure. The gray dotted arrows guide the shift of the peaks. All measurements are conducted at room temperature.

Figure S3 shows the evolution of PL spectrum of ReS₂ crystal with applied pressure (0-14 GPa) for different configurations, where the PL peak intensities change with pressure, and are quenched above 14 GPa. In addition, we also observe distinctive changes of peak width and peak position with pressure for H and V configurations, offering important clues for analyzing the electronic structure of ReS₂ crystals. Specifically, in the H configurations (Figures S3a & S3b), all five excitonic peaks show red shift with pressure, with a change of pressure coefficients ($\partial E/\partial P$) at 3.20 GPa. This corresponds to the different response of 1T' phase (< 3.20 GPa) and distorted 1T' (> 3.20 GPa) to applied pressure. Further, the indirect excitonic peak and the high-energy excitonic peak X³_{1/2} disappear at 3.20 GPa (Figures S3e & S3f), suggesting a transition from the indirect bandgap to direct bandgap in the ReS₂ crystal. Interestingly, such

transition takes place at 5.12 GPa in the V configurations (Figures S3c & S3d and Figures S3g & S3h), which is in excellent agreement with the phase transition processes observed in previous Raman results.

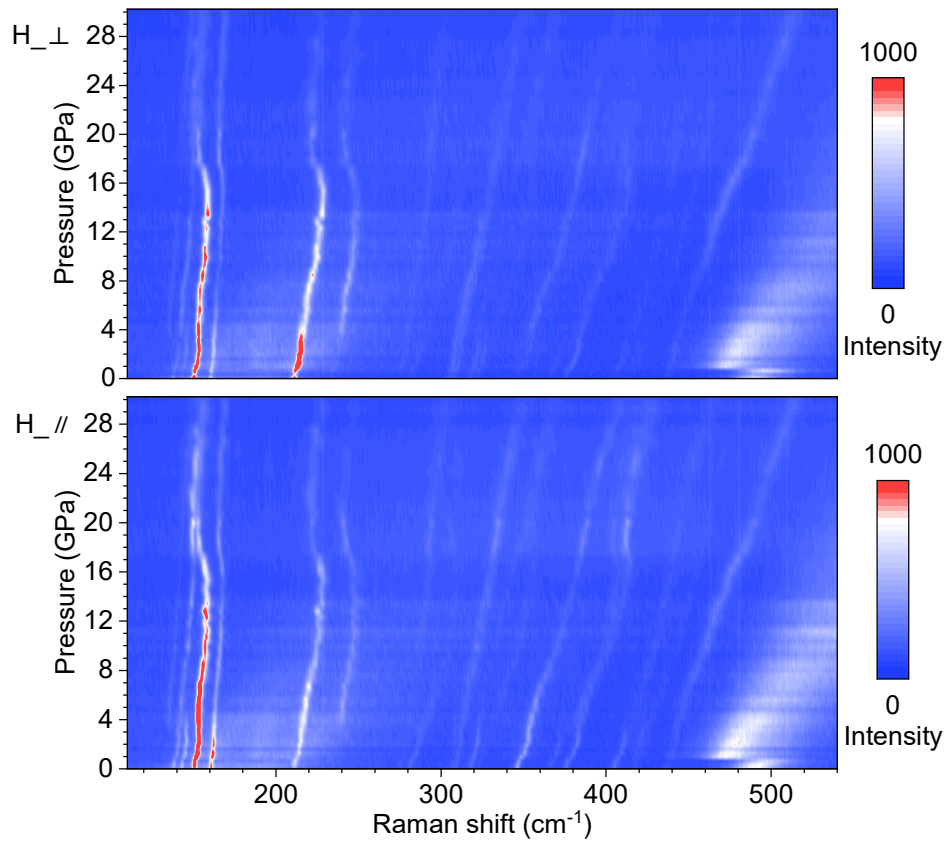


Figure S4. Evolution of Raman spectrum of ReS_2 crystal in the frequency range 110-540 cm^{-1} from ambient to 30.24 GPa for H configuration.

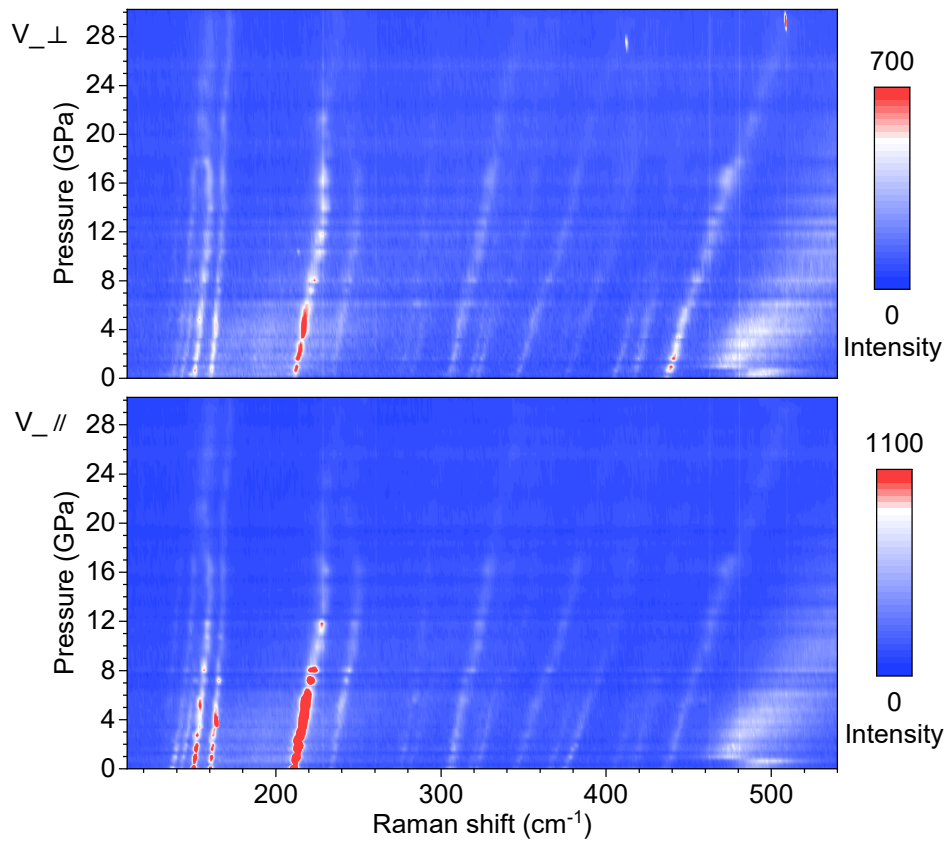


Figure S5. Evolution of Raman spectrum of ReS₂ crystal in the frequency range 110-540 cm⁻¹ from ambient to 30.24 GPa for V configuration.

Peak	$f(\text{cm}^{-1})$	Mode	H_// (GPa)	H_⊥ (GPa)	V_// (GPa)	V_⊥ (GPa)
α	~137	-	3.20 - 25.60	3.20 - 25.60	5.12 - 17.76	5.12 - 17.76
1	137	A _g -like	0 - 20.00	0 - 20.00	0 - 17.76	0 - 17.76
2	142	E _g -like	0 - 3.20	0 - 3.20	0 - 9.92	0 - 9.92
10	305	E _g -like	0 -	0 -	0 - 5.12	0 - 5.12
11	316	A _g -like	0 -	0 -	0 - 5.12	0 - 5.12
12	320	A _g -like	0 - 20.00	0 - 20.00	0 - 17.76	0 - 17.76
13	344	E _g -like	0 -	0 -	0 - 17.76	0 -
14	365	A _g -like	0 - 3.20	0 - 3.20	0 - 5.12	0 - 5.12
15	374	E _g -like	0 - 11.84<	0 - 11.84<	0 - 17.76	0 - 17.76
16	403	A _g -like	0 -	0 - 25.60	0 - 5.12	0 - 9.92
17	415	A _g -like	0 - 20.00	0 - 25.60	0 - 5.12	0 - 9.92

Table S2. The emerging (red), splitting (green) and vanishing (black) behaviors of Raman peaks for H_//, H_⊥, V_// and V_⊥ configurations at different pressure values. “<” represents the splitting behavior of the peak after this pressure. The hyphens indicate the blue-shift Raman peaks without splitting or vanishing behavior in the measured pressure range.